

# Comparative analysis of two discretizations of Ricci curvature for complex networks

Areejit Samal,<sup>1</sup> R.P. Sreejith,<sup>1</sup> Jiao Gu,<sup>2</sup> Shiping Liu,<sup>3,\*</sup> Emil Saucan,<sup>4,5,†</sup> and Jürgen Jost<sup>6,7,‡</sup>

<sup>1</sup>*The Institute of Mathematical Sciences, Homi Bhabha National Institute, Chennai, India*

<sup>2</sup>*Jiangnan University, Wuxi, P.R. China*

<sup>3</sup>*School of Mathematical Sciences, University of Science and Technology of China, Hefei, P.R. China*

<sup>4</sup>*Department of Applied Mathematics, ORT Braude College, Karmiel, Israel*

<sup>5</sup>*Department of Electrical Engineering, Technion, Israel Institute of Technology, Haifa, Israel*

<sup>6</sup>*Max Planck Institute for Mathematics in the Sciences, Leipzig, Germany*

<sup>7</sup>*The Santa Fe Institute, Santa Fe, New Mexico, USA*

We have performed an empirical comparison of two distinct notions of discrete Ricci curvature for graphs or networks, namely, the Forman-Ricci curvature and Ollivier-Ricci curvature. Importantly, the two discretizations of the Ricci curvature, Forman-Ricci and Ollivier-Ricci, were developed based on different properties of the classical smooth notion, and thus, the two notions shed light on different aspects of network structure and behavior. Nevertheless, our extensive computational analysis in wide-range of both model and real-world networks shows that the two discretizations of Ricci curvature are statistically well correlated. Besides the potential theoretical implications of these observations, the close relationship between the two discretizations has practical implications whereby Forman-Ricci curvature can be employed in place of Ollivier-Ricci curvature for faster computation in larger networks whenever coarse analysis suffices.

## I. INTRODUCTION

One of the central quantities, and arguably the most important one, associated to a Riemannian metric is the Ricci tensor. In Einstein's field equations, the energy-momentum tensor yields the Ricci tensor, and this determines the metric of space-time. In Riemannian geometry, the importance of the Ricci tensor came to the fore in particular through the work of Gromov, see for instance [1]. The Ricci flow, introduced by Hamilton [2], culminated in the work of Perelman [3, 4] which solved the Poincaré and the more general Geometrization Conjecture for three-dimensional manifolds. On the other hand, there have been important developments extending the notion of Ricci curvature axiomatically to metric spaces more general than Riemannian manifolds, see for instance [5–7]. More precisely, one identifies metric properties on a Riemannian manifold that can be formulated in terms of local quantities, like the growth of volumes of distance balls, transportation distances between balls, divergence of geodesics, meeting probabilities of coupled random walks and the like, that on Riemannian manifolds are implied by, or even equivalent to Ricci curvature inequalities. When such metric properties then are satisfied on some metric space, one says that the space satisfies the corresponding generalized Ricci curvature inequality. This research paradigm has been remarkably successful, and the geometry of metric spaces with such inequalities is currently a very active and fertile field of mathematical research, see for instance [8]. Of course, while on Riemannian manifolds various such properties are equivalent to Ricci curvature inequalities and therefore also to each other, the various such quantities and corresponding definitions of Ricci curvature bounds of the axiomatic approach need no longer be equivalent on general metric spaces.

There is also an older line of research [9] that searches for the discretization of Ricci curvature on graphs and more general objects with a combinatorial structure. Here, one has exact quantities instead of inequalities only as in the aforementioned research. This has recently gained momentum, spurred by Perelman's [3, 4] ground-breaking results. One elegant approach is by Chow and Luo [10] based on circle packings which lent itself to many practical applications in graphics, medical imaging and communication networks [11–13]. On the other hand, the above mentioned approach to Ricci curvature inequalities on metric spaces led to Ollivier's construction [14–17] which proved to be suitable for modelling complex networks as well as rendering interesting theoretic results with potential of future applications [18–24]. Still another approach to the discretization of Ricci curvature on networks, and more generally, on polyhedral complexes, is due to Forman [25]. In recent work [26–30], we have started to systematically explore Forman-Ricci curvature on complex networks. A crucial advantage of Forman-Ricci curvature is that, while it also captures important geometric properties of networks, it is far simpler to evaluate on large networks than Ollivier-Ricci curvature. In this contribution, we show via extensive empirical analysis of both model and real networks

\* [spliu@ustc.edu.cn](mailto:spliu@ustc.edu.cn)

† [semil@ee.technion.ac.il](mailto:semil@ee.technion.ac.il)

‡ [jost@mis.mpg.de](mailto:jost@mis.mpg.de)

that Forman-Ricci curvature is strongly correlated to Ollivier-Ricci curvature. This makes Forman-Ricci curvature a preferential tool for the analysis of very large networks with various practical applications.

Although we show here that Forman-Ricci curvature is strongly correlated to Ollivier-Ricci curvature in complex networks, one should not construe from this observation that we introduce Forman-Ricci curvature as a substitute (and certainly not as a “proxy” [31]) for Ollivier-Ricci curvature. As we have already mentioned above, and as we shall further explain in the following section, the two types of curvature capture quite different aspects of network behavior. Therefore, given that the specific definitions of both Ollivier’s and Forman’s discretizations of Ricci curvature prescribe some of their respective essential properties that have important consequences in certain significant applications, we shall detail these definitions and not restrict ourselves to the mere technical defining formulas.

Amongst the most powerful tools developed recently for the study of complex networks [32–38], geometric tools [15, 18–21, 23, 24, 26, 39–41], and mainly curvature, allow us to gain deep insights into the structure, properties and evolution of networks. It is in the very nature of discretization of differential geometric properties that each such discrete notion sheds a different light and understanding upon the studied object (e.g., a graph or a network). In particular, Ollivier’s curvature is related to clustering and network coherence (via the distribution of the eigenvalues of the graph Laplacian), giving insights into the global and local structure of networks. In contrast, Forman’s curvature captures the geodesics dispersal property and also gives information on the algebraic topological structure of the network. Furthermore, Forman’s curvature, as noted earlier, is simple to compute, and can easily be extended to analyze both directed networks and hyper-networks [26–29]. Given the contrast between the two discretizations of Ricci curvature at hand, their essential statistical equivalence is quite surprising and encouraging, thus certainly deserving investigation and measurement. Moreover, the fact that both types of curvature admit natural Ricci curvature flows [12, 29], that allows for the study of long time evolution and prediction of networks, further increases the relevance and importance of such an investigation for the better understanding of the structure and development of complex networks.

In Riemannian geometry, Ricci curvature plays such an important role for several reasons, one of them being that it has the same number of degrees of freedom as the metric tensor, since both are symmetric two-tensors. Thus, the Ricci tensor should encode all the essential properties of a Riemannian metric. Similarly, it is an emerging principle that Ricci curvature, because it evaluates edges instead of vertices, also captures the basic structural aspects of a network. Both Ollivier-Ricci and Forman-Ricci curvature assign a number to each edge of a (possibly weighted and directed) network that encodes local geometric properties in the vicinity of that edge. We highlight that *edges* are what networks are made of as the *vertices* alone do not yet constitute a network.

## II. DISCRETE RICCI CURVATURES ON NETWORKS

We briefly present here the geometric meaning of the notion of Ricci curvature, as well as the two discretizations considered herein. For other discretizations of this type of curvature and their applications, see for instance [12].

### A. Ricci curvature

In Riemannian geometry curvature measures the deviation of the manifold from being locally Euclidean. Ricci curvature quantifies that deviation for tangent directions. It controls the average dispersion of geodesics around that direction. It also controls the growth of the volume of distance balls and spheres. In fact, these two properties are related, as can be seen from the following formula [42];

$$V_\alpha(\varepsilon) = d\alpha \varepsilon^{n-1} \left( 1 - \frac{\text{Ric}(\mathbf{v})}{3} \varepsilon^2 + o(\varepsilon^2) \right). \quad (1)$$

Here,  $n$  is the dimension of the Riemannian manifold in question, and  $V_\alpha(\varepsilon)$  is the  $(n-1)$ -volume generated within an  $n$ -solid angle  $d\alpha$  by geodesics of length  $\varepsilon$  in the direction of the vector  $\mathbf{v}$  (i.e., it controls the growth of measured angles). Thus, Ricci curvature controls both divergence (of geodesics) and (volume) growth (Figure 1). In dimension  $n = 2$ , Ricci curvature reduces to the classical *Gauss curvature*, and can therefore be easily visualized.

As we shall see, the two definitions for discrete Ricci curvature, those of Ollivier and Forman, that we shall consider in this paper, for networks capture different properties of the classical (smooth) notion: Forman’s definition expresses dispersal (diffusion), while Ollivier’s definition compares the averaged distance between balls to the distance between their centers. Thus, the two definitions lead to different generalization of classical results regarding Ricci curvature. In this respect, Ollivier’s version seems to be advantageous, since, in addition to certain geometric properties, analytic inequalities also hold, whereas Forman’s version encapsulates mainly the topology of the underlying space.

Nevertheless, in our specific context, as we shall show in the sequel, Ollivier's and Forman's definitions are strongly correlated and therefore, for the empirical analysis of large networks, at least in a first approximation, from the analysis of one of the definitions, one can also make inferences about the properties encoded by the other. Thus, for instance, Ollivier's curvature is, by its very definition, excellently suited to capture diffusion and stochastic properties of a given network. Unfortunately, the computations required might prove prohibitive for a realistically large complex networks. However, due to its simple, combinatorial formula (see below), Forman's curvature is easy and fast to compute. Given the basic equivalence, at least on a statistical level, between these two notions, one can therefore determine, at least in first approximation, many properties encapsulated by Ollivier's curvature via simple computations with Forman's curvature. However, for a finer analysis, each of the two discrete Ricci curvatures should be employed in the context that best befits the geometrical phenomenology it encapsulates.

## B. Ollivier-Ricci curvature

Ollivier's approach [14–17] interprets formula (1) as follows: If a small ball (of radius  $\varepsilon$ )  $B_x$  centered at  $x$  is mapped, via optimal transport to  $B_y$ , a corresponding ball centered at  $y$ , where  $d(x, y) = \delta$ , then the transportation cost is:

$$\delta \left( 1 - \frac{\varepsilon^2}{2(n+2)} \text{Ric}(v) + O(\varepsilon^3 + \varepsilon^2 \delta) \right), \quad (2)$$

where  $\varepsilon, \delta \rightarrow 0$ .

Thus, we can *synthetically* characterize Ricci curvature by the following phrase: “In positive (negative) curvature, balls are closer (farther) than their centers are” ([17]). Balls are given by their volume measures, and in fact, one may define a transportation distance for any two (normalized) measures. In this sense, Ollivier's notion compares the distance between the centers of their balls with that between their measures (Figure 2). For the distance between the centers, one takes (of course) the given metric of the underlying space, i.e., manifold, mesh, network, etc. As for the distance between measures, there is a natural choice, the Wasserstein transportation metric  $W_1$  [43]. More formally, Ollivier's curvature is defined as:

$$\kappa(x, y) = 1 - \frac{W_1(m_x, m_y)}{d(x, y)}; \quad (3)$$

where  $m_x, m_y$  represent the measures of the balls around  $x$  and  $y$ , respectively.

In the Riemannian setting, Ollivier's definition reduces to the classical one. More precisely, if  $M^n$  is a Riemannian manifold, with its natural measure  $d\text{Vol}$ , then for  $d(x, y)$  small enough and  $v$  the unit tangent vector at  $x$  on the geodesic  $\overline{xy}$

$$\kappa(x, y) = \frac{\varepsilon^2}{2(n+2)} \text{Ric}(v) + O(\varepsilon^3 + \varepsilon^2 d(x, y)).$$

*Implementation:* The Wasserstein distance between two vertices in a network depends on the triangles, quadrangles and pentagons that they are contained in (see for instance, [21, 44]). It can also be computed in terms of random walks on a graph, where one has the choice between the *lazy* [23] and the *non-lazy* [21] random walk. While the two variants are clearly equivalent from a theoretical viewpoint, the choices may render differences in the implementation. In this work, we have used the lazy random walk option within the open-source implementation (<https://github.com/matsengrp/gricci/blob/master/code.py>) of Ollivier-Ricci curvature, originally developed by P. Romon and improved by E. Madsen, within SageMath (<http://www.sagemath.org/>) software for our computations.

## C. Forman-Ricci curvature

Forman's definition [25] is conceptually quite different from Ollivier's. To begin with, Forman's definition works in the framework of *weighted CW cell complexes*, which are of fundamental importance in topology and include both polygonal meshes and weighted graphs, rather than that of Markov chains and metric measure spaces, as Ollivier's does. In the setting of weighted CW cell complexes, it develops an abstract version of a classical formula in differential geometry or geometric analysis, the so called *Bochner-Weitzenböck* formula (see, for instance [45]), that relates curvature to the classical (Riemannian) Laplace operator.

Forman [25] derived an analogue of the Bochner-Weitzenböck formula that holds in the setting of *CW* complexes. In the 1-dimensional case, i.e. that of graphs or networks, it takes the following form:

$$F(e) = w_e \left( \frac{w_{v_1}}{w_e} + \frac{w_{v_2}}{w_e} - \sum_{e_{v_1} \sim e, e_{v_2} \sim e} \left[ \frac{w_{v_1}}{\sqrt{w_e w_{e_{v_1}}}} + \frac{w_{v_2}}{\sqrt{w_e w_{e_{v_2}}}} \right] \right). \quad (4)$$

Since edges in the discrete setting of networks naturally correspond to vectors or directions in the smooth context, this formula represents, indeed, a discretization of Ricci curvature.

In the combinatorial case, i.e. for  $\omega(e) = \omega(v) = 1$ ,  $e \in E(G)$ ,  $v \in V(G)$ , where  $E(G)$  and  $V(G)$  represent the set of edges and vertices, respectively, in graph  $G$ , the above formula reduces to the quite simple and intuitive expression:

$$F(e) = 2 - \sum_{v \sim e} \deg(v). \quad (5)$$

This simple case captures the role of Ricci curvature as a measure of the flow through an edge and illustrates how Ricci curvature captures the “social behavior” of geodesics dispersal depicted in Figure 1.

From a graph, one may construct two-dimensional polyhedral complexes by inserting a two-dimensional simplex into any connected triple of vertices, a tetragon into any cycle of length 4, a pentagon into a cycle of length 5, and so on. This is natural, if, for instance, one wants to represent higher order correlations between vertices. Again, Forman’s scheme assigns a Ricci curvature to such a complex, via the formula, which also includes possible weights  $\omega$  of simplices, edges, and vertices:

$$F(e) = \omega(e) \left[ \left( \sum_{e < f} \frac{\omega(e)}{\omega(f)} + \sum_{v < e} \frac{\omega(v)}{\omega(e)} \right) - \sum_{\hat{e} \parallel e} \left| \sum_{\hat{e}, e < f} \frac{\sqrt{\omega(e) \cdot \omega(\hat{e})}}{\omega(f)} - \sum_{v < e, v < \hat{e}} \frac{\omega(v)}{\sqrt{\omega(e) \cdot \omega(\hat{e})}} \right| \right]; \quad (6)$$

where  $\sigma < \tau$  means that  $\sigma$  is a face of  $\tau$ , and where  $\parallel$  signifies parallelism, i.e. the two cells have a common “parent” (higher dimensional face) or a common “child” (lower dimensional face), but not both a common parent and common child. In particular, for unweighted networks, i.e.  $\omega(f) = \omega(e) = \omega(v) = 1$ ,  $\forall f \in F(G)$ ,  $e \in E(G)$ ,  $v \in V(G)$ , where  $F(G)$ ,  $E(G)$  and  $V(G)$  represent the set of faces, edges and vertices, respectively, in graph  $G$ , the terms reduce to the simple counting of adjacent parents and children, respectively, and we get:

$$\begin{aligned} F(e) &= \#\{f > e\} + \#\{v < e\} - (\#\{\hat{e} | \hat{e} \parallel e\} - \#\{v | v \sim e, v \sim \hat{e}, e \parallel \hat{e}\}) \\ &= \#\{f > e\} - \#\{\hat{e} | \hat{e} \parallel e\} + 2. \end{aligned} \quad (7)$$

When we have only triangular faces, but no polygons with more than three vertices, the last term in this formula becomes 0, because for triangular faces, no parallel edges to  $e$  exist, and hence the corresponding set is empty.

#### D. Ollivier’s vs. Forman’s Ricci curvature: A first comparison

The two types of Ricci curvature, Ollivier-Ricci and Forman-Ricci, express different geometric properties of a network, and they can therefore be quite different from each other for specific networks. For example, consider a complete graph on  $n$  vertices where any two vertices share  $n - 2$  neighbors, and therefore, the corresponding balls largely overlap. The transportation distance between any two vertices in such a graph is thus very small, and thus, the Ollivier-Ricci curvature (Eq. 3) is almost one for large  $n$ , the largest possible value. On the other hand, the degree of any vertex is  $n - 1$  in such a graph, and therefore, the Forman-Ricci curvature (Eq. 5) takes the most negative possible value. Thus, for such graphs, the two types of Ricci curvature behave in opposite ways. Thus, it is not surprising that in small, specific cases, they can numerically diverge from each other, as exemplified in Figure 4. Nevertheless, the experimental results that we present in the following sections show that, statistically, Ollivier-Ricci and Forman-Ricci curvatures for networks correlate quite well. Thus, in the classes of theoretical and empirical networks that we have investigated, large degrees of the vertices bounding an edge do not statistically correlate strongly with large fractions of triangles or other short loops containing these vertices. Still we would like to remark that if we modify Forman-Ricci definition by inserting simplices into triangles, i.e., to say, correlations between triplets of nodes, as suggested above (Eq. 7), then the two types of curvature are better correlated even at “small scale”, because in that case, triangles of vertices no longer contribute negatively to Forman-Ricci curvature.

### III. BENCHMARK DATASET OF COMPLEX NETWORKS

We have considered three models, Erdős-Rényi (ER) [46], Watts-Strogatz (WS) [33] and Barabási-Albert (BA) [34], of undirected networks. The ER model [46] is the prototype for random networks. The ER model produces an ensemble of random graphs  $G(n, p)$  where  $n$  is the number of vertices and  $p$  is the probability that each possible edge exists between any pair of vertices in the network. The WS model [33] is the prototype for small-world networks which exhibit both a high clustering coefficient and a small average path length. In the WS model, an initial regular graph is generated with  $n$  vertices on a ring lattice with each vertex connected to its  $k$  nearest neighbours. Subsequently an endpoint of each edge in the regular ring graph is rewired with probability  $\beta$  to a new vertex selected from all the vertices in the network with a uniform probability. The BA model [34] is the prototype for scale-free networks which exhibit a power-law degree distribution. In the BA model, an initial graph is generated with  $m_0$  vertices. Thereafter, a new vertex is added to the initial graph at each step of this evolving network model such that the new vertex is connected to  $m \leq m_0$  existing vertices, selected with a probability proportional to their degree. The BA model thus implements a preferential attachment scheme where high-degree vertices have a higher chance of acquiring new edges than low-degree vertices.

We have also considered eight widely-studied real undirected networks. These are three communication networks (described below), the Euro road network [47], the US Power Grid network [48] and an Email communication network [49]. In the Euro road network, the 1174 vertices are cities in Europe, and the 1417 edges are roads in the international E-road network linking them. In the US Power Grid network, the 4941 vertices are generators or transformers or substations in the western states of the US, and the 6594 edges are power supply lines linking them. In the Email communication network, the 1133 vertices are users in the University Rovira i Virgili in Tarragona in Spain, and the 5451 edges represent direct communication between them. We have considered one social network, the Hamsterster friendship network, where the 2426 vertices are users of hamsterster.com, and the 16631 edges represent friendship or family links between them. We have also considered a linguistic network, an adjective-noun adjacency network [50], where the 112 vertices are nouns or adjectives, and the 425 edges represent their presence in adjacent positions in the novel David Copperfield by Charles Dickens. We have considered three biological networks, the yeast protein interaction network [51], the PDZ domain interaction network [52] and the human protein interaction network [53]. In the yeast protein interaction network, the 1870 vertices are proteins in yeast *Saccharomyces cerevisiae*, and the 2277 edges are interactions between them. In the PDZ domain interaction network, the 212 vertices are proteins, and the 244 edges are PDZ-domain mediated interactions between proteins. In the human protein interaction network, the 3133 vertices are proteins, and the 6726 edges are interactions between human proteins as captured in an earlier release of the proteome-scale map of human binary protein interactions. The eight empirical networks analyzed here were downloaded from the KONECT [54] database.

In earlier work [26, 28], we had characterized the Forman-Ricci curvature of edges and vertices in the above-mentioned networks. In the present work, we have compared the Forman-Ricci (FR) curvature and Ollivier-Ricci (OR) curvature of edges and vertices in those networks.

### IV. RESULTS AND DISCUSSION

#### A. Comparison between Forman-Ricci and Ollivier-Ricci curvature in model and real networks

We have compared the FR and OR curvature of edges in model and real networks. In random ER networks, we find a very high positive correlation between FR and OR curvature of edges (Table I; Figure 5). In small-world WS and scale-free BA networks, we find a significantly high positive correlation between FR and OR curvature of edges (Table I; Figure 5). We have also computed the FR and OR curvature of edges in eight real-world networks. In most real-world networks considered here, we find a moderate to high positive correlation between FR and OR curvature of edges (Table I; Figure 5). Thus, in both model and real networks, we observe a positive correlation between FR and OR curvature of edges.

From the definition of the FR and OR curvature of edges, it is straightforward to define FR and OR curvature of vertices in networks [24, 28]. Note that the definition of FR and OR curvature of vertices in networks [24, 28] is analogous to scalar curvature in Riemannian geometry [45]. We have also compared the FR and OR curvature of vertices in model and real networks. In random ER and small-world WS networks, we find a very high positive correlation between FR and OR curvature of vertices (Table I). In scale-free BA networks, we find a high positive correlation between FR and OR curvature of vertices (Table I). In the real-world networks considered here, we find a high positive correlation between FR and OR curvature of vertices (Table I). Thus, in both model and real networks, we also observe a significant positive correlation between FR and OR curvature of vertices.

Importantly, we find that the correlation between FR and OR curvature of vertices is higher than FR and OR curvature of edges in model and real networks (Table I). Furthermore, we find a high positive correlation between FR and OR curvature of vertices in Email communication network where only a weak positive correlation exists between FR and OR curvature of edges (Table I). In a nut shell, although the two discretizations of Ricci curvature, FR and OR, capture different geometrical properties, our empirical analysis finds a significant positive correlation in complex networks. We highlight that the observed positive correlation between FR and OR curvature also transcends different types of real networks spanning communication, social, linguistic and biological networks.

### B. Comparison of Forman-Ricci and Ollivier-Ricci curvature with other edge-based measures

We emphasize that FR and OR curvature are edge-based measures of complex networks. We compared FR and OR curvature with three other edge-based measures, edge betweenness centrality [37, 55, 56], embeddedness [57] and dispersion [58], for complex networks. Edge betweenness centrality [37, 55, 56] measures the number of shortest paths that pass through an edge in a network. Edge betweenness centrality can be used to identify bottlenecks for flows in network. Embeddedness [57] of an edge quantifies the number of neighbors that are shared by the two vertices anchoring the edge under consideration in the network. Embeddedness is a measure to quantify the strength of ties in social networks. Dispersion [58] quantifies the extent to which the neighbours of the two vertices anchoring an edge are not themselves well connected [58]. Dispersion is a measure to predict romantic relationships in social networks.

In model networks, we find that both FR and OR curvature have significant negative correlation with edge betweenness centrality (Table II). In real networks considered here, we find that FR curvature has a weak to moderate negative correlation with edge betweenness centrality while OR curvature has moderate to high negative correlation with edge betweenness centrality (Table II). Furthermore, in the real networks considered here, we observe a higher negative correlation between OR curvature and edge betweenness centrality in comparison to FR curvature and edge betweenness centrality (Table II). This may be explained by the fact that OR curvature is also affected by cycles of length 4 and 5 containing the two vertices of an edge, and these are relevant for edge betweenness centrality.

In random ER and small-world WS networks, we find that FR curvature has no correlation with embeddedness or dispersion, while in scale-free BA networks, FR curvature has moderate negative correlation or weak negative correlation with embeddedness or dispersion, respectively (Table II). In random ER and scale-free BA networks, we find that OR curvature has no correlation with embeddedness or dispersion, while in small-world WS networks, OR curvature has high positive correlation or weak positive correlation with embeddedness or dispersion, respectively (Table II). Among real networks, we find that FR curvature has no correlation to high negative correlation with embeddedness or dispersion depending on the considered network (Table II). Similarly, among real networks, we find that OR curvature can have anything between no and high positive correlation with embeddedness or dispersion depending on the considered network (Table II). Thus, both FR and OR curvature do not have a consistent relationship with embeddedness or dispersion in model and real networks.

### C. Comparison of Forman-Ricci and Ollivier-Ricci curvature with vertex-based measures

We compared FR and OR curvature of vertices with three other vertex-based measures, degree, clustering coefficient [33, 59] and betweenness centrality [37, 55], in a network. Vertex degree gives the number of edges incident to that vertex in a network. The clustering coefficient [33, 59] of a vertex quantifies the number of edges that are realized between the neighbours of the vertex divided by the number of edges that could possibly exist between the neighbours of the vertex in the network. We remark that the clustering coefficient has been proposed as a measure to quantify the curvature of networks [39]. Betweenness centrality [37, 55] of a vertex quantifies the fraction of shortest paths between all pairs of vertices in the network that pass through that vertex.

Not surprisingly, we find that both FR and OR curvature of vertices have high negative correlation with degree in model networks as well as in real networks (Table III). After all, the vertex degree is intrinsic in the definition of the FR or OR curvature of a vertex as it appears implicitly in the sum over adjacent edges in the defining formula. In random ER networks, we find that FR curvature of vertices has no correlation with the clustering coefficient, while in small-world WS and scale-free BA networks, FR curvature of vertices has weak negative correlation and moderate negative correlation, respectively, with the clustering coefficient (Table III). In random ER networks, we find that OR curvature of vertices has no correlation with the clustering coefficient, while in small-world WS and scale-free BA networks, OR curvature of vertices has weak positive correlation and weak negative correlation, respectively, with the clustering coefficient (Table III). Among real networks, we find that FR curvature of vertices has weak positive correlation to no correlation to moderate negative correlation with the clustering coefficient depending on the considered network (Table III). Similarly, among real networks, we find that OR curvature of vertices has high

positive correlation to no correlation to moderate negative correlation with the clustering coefficient depending on the considered network (Table III). Thus, both FR and OR curvature of vertices do not have a consistent relationship with the clustering coefficient in model and real networks. In model networks, we find that both FR and OR curvature of vertices have high negative correlation with betweenness centrality (Table III). In real networks considered here, we find that both FR and OR curvature of vertices have negative correlation with betweenness centrality (Table III). Thus, both FR and OR curvature of vertices has negative correlation with betweenness centrality in model and real networks.

#### D. Relative importance of Forman-Ricci and Ollivier-Ricci curvature for topological robustness of networks

We investigated the relative importance of FR and OR curvature of edges for the large-scale connectivity of networks by removing edges based on the following criteria: random order, increasing order of the FR curvature of an edge, increasing order of the OR curvature of an edge, and decreasing order of edge betweenness centrality. We employ a global network measure, communication efficiency [60], to quantify the effect of removing edges on the large-scale connectivity of networks. Note that communication efficiency captures the resilience of a network to failure in the face of perturbations. In both model and real networks, we find that removing edges based on increasing order of FR curvature or increasing order of OR curvature or decreasing order of edge betweenness centrality leads to faster disintegration in comparison to the random removal of edges (Figure 6). Furthermore, in both model and real networks, removing edges based on increasing order of OR curvature or decreasing order of edge betweenness centrality typically leads to faster disintegration in comparison to removing edges based on increasing order of FR curvature (Figure 6). Also, in both model and real networks, removing edges based on increasing order of OR curvature typically leads to slightly faster disintegration in comparison to removing edges based on decreasing order of edge betweenness centrality (Figure 6).

We also investigated the relative importance of FR and OR curvature of vertices for the large-scale connectivity of networks by removing vertices based on following criteria: random order, increasing order of the FR curvature of a vertex, increasing order of the OR curvature of a vertex, decreasing order of betweenness centrality of a vertex, decreasing order of vertex degree, and decreasing order of clustering coefficient of a vertex. In both model and real networks, we find that removing vertices based on increasing order of FR curvature or increasing order of OR curvature or decreasing order of betweenness centrality or decreasing order of degree leads to faster disintegration in comparison to the random removal of vertices (Figure 7). Furthermore, in both model and real networks, removing vertices based on increasing order of OR curvature typically leads to faster disintegration in comparison to removing edges based on increasing order of FR curvature (Figure 7). Also, in both model and real networks, removing edges based on increasing order of OR curvature typically leads to at least slightly faster disintegration in comparison to removing edges based on any other measure (Figure 7). In summary, vertices or edges with highly negative OR curvature are more important than vertices or edges with highly negative FR curvature for maintaining the large-scale connectivity of networks.

## V. CONCLUSIONS

We have performed an empirical investigation of two discrete notions of Ricci curvature, Ollivier’s Ricci curvature and Forman’s Ricci curvature, in a number of model and real-world networks. The two discretizations of Ricci curvature were derived using different theoretical considerations and methods, and thus convey insights into quite different geometrical properties and behaviors of complex networks. Specifically, Ollivier-Ricci curvature captures clustering and coherence in networks while Forman-Ricci curvature captures dispersal and topology. Still, our results obtained in a wide-range of both model and real-world networks, consistently demonstrate that the two types of Ricci curvature in networks are statistically well correlated. The immediate benefit of this realization is that one can compute Forman-Ricci curvature in large networks to gain some first preliminary insight into the computationally much more demanding Ollivier-Ricci curvature. Moreover, our empirical observations on the correlation between these two different notions of Ricci curvature in networks warrant deeper investigation in the future.

We remark that while the present manuscript was under final stages of submission, a preprint [61] devoted to comparison problem on biological networks appeared on Arxiv server, independently from our present study.

## ACKNOWLEDGMENTS

ES and AS thank the Max Planck Institute for Mathematics in the Sciences, Leipzig, for their warm hospitality. AS would like to acknowledge support from Max Planck Society, Germany, through the award of a Max Planck Partner Group in Mathematical Biology.

---

[1] M. Gromov, *Structures métriques pour les variétés riemanniennes* (Rédigé par J. Lafontaine and P. Pansu. Cedic-Nathan, Paris, 1980).

[2] R. Hamilton, A.M.S. Contemp. Math. **71**, 237 (1986).

[3] G. Perelman, arXiv math/0211159 (2002).

[4] G. Perelman, arXiv math/0303109 (2003).

[5] D. Bakry, I. Gentil, and M. Ledoux, *Analysis and geometry of Markov diffusion operators* (Springer Nature, 2014).

[6] J. Lott and C. Villani, Annals of Mathematics , 903 (2009).

[7] K. Sturm, Acta mathematica **196**, 65 (2006).

[8] F. Bauer, B. Hua, J. Jost, S. Liu, and G. Wang, in *Modern Approaches to Discrete Curvature* (Springer, 2017) pp. 1–62.

[9] D. A. Stone, Illinois Journal of Mathematics **20**, 12 (1976).

[10] B. Chow and F. Luo, Journal of Differential Geometry **63**, 97 (2003).

[11] M. Jin, J. Kim, and X. D. Gu, in *Mathematics of Surfaces XII* (Springer, 2007) pp. 209–232.

[12] D. Gu and E. Saucan, Geometry **2013** (2013).

[13] J. Gao, X. D. Gu, and F. Luo, “Discrete ricci flow for geometric routing,” in *Encyclopedia of Algorithms*, edited by M.-Y. Kao (Springer Berlin Heidelberg, Berlin, Heidelberg, 2014) pp. 1–8.

[14] Y. Ollivier, Comptes Rendus Mathématique **345**, 643 (2007).

[15] Y. Ollivier, Journal of Functional Analysis **256**, 810 (2009).

[16] Y. Ollivier, Probabilistic approach to geometry **57**, 343 (2010).

[17] Y. Ollivier, Analysis and Geometry of Metric Measure Spaces: Lecture Notes of the 50th Séminaire de Mathématiques Supérieures (SMS), Montréal, 2011 , 197 (2013).

[18] Y. Lin and S. Yau, Math. Res. Lett **17**, 343 (2010).

[19] Y. Lin, L. Lu, S. Yau, *et al.*, Tohoku Mathematical Journal **63**, 605 (2011).

[20] F. Bauer, J. Jost, and S. Liu, Mathematical research letters **19**, 1185 (2012).

[21] J. Jost and S. Liu, Discrete & Computational Geometry **51**, 300 (2014).

[22] B. Loisel and P. Romon, Axioms **3**, 119 (2014).

[23] C. Ni, Y. Lin, J. Gao, X. D. Gu, and E. Saucan, in *IEEE Conference on Computer Communications (INFOCOM)* (IEEE, 2015) pp. 2758–2766.

[24] R. Sandhu, T. Georgiou, E. Reznik, L. Zhu, I. Kolesov, Y. Senbabaoglu, and A. Tannenbaum, Scientific Reports **5** (2015).

[25] R. Forman, Discrete and Computational Geometry **29**, 323 (2003).

[26] R. Sreejith, K. Mohanraj, J. Jost, E. Saucan, and A. Samal, Journal of Statistical Mechanics: Theory and Experiment , P063206 (2016).

[27] R. P. Sreejith, J. Jost, E. Saucan, and A. Samal, arXiv preprint arXiv:1605.04662 (2016).

[28] R. Sreejith, J. Jost, E. Saucan, and A. Samal, Chaos, Solitons & Fractals **101**, 50 (2017).

[29] M. Weber, E. Saucan, and J. Jost, Journal of Complex Networks , cnw030 (2017).

[30] E. Saucan, A. Samal, M. Weber, and J. Jost, MPI MIS preprint 34/2017 (2017).

[31] S. Pal, F. Yu, T. J. Moore, R. Ramanathan, A. Bar-Noy, and A. Swami, arXiv preprint arXiv:1710.01724 (2017).

[32] S. Wasserman and K. Faust, *Social network analysis: Methods and applications*, Vol. 8 (Cambridge University Press, 1994).

[33] D. J. Watts and S. H. Strogatz, Nature **393**, 440 (1998).

[34] A. L. Barabási and R. Albert, Science **286**, 509 (1999).

[35] R. Albert and A. L. Barabási, Reviews of Modern Physics **74**, 47 (2002).

[36] J. Feng, J. Jost, and M. Qian, *Networks: from biology to theory* (Springer, 2007).

[37] M. Newman, *Networks: an introduction* (Oxford University Press, 2010).

[38] S. Fortunato, Physics Reports **486**, 75 (2010).

[39] J. Eckmann and E. Moses, Proceedings of the National Academy of Sciences **99**, 5825 (2002).

[40] Z. Wu, G. Menichetti, C. Rahmede, and G. Bianconi, Scientific Reports **5** (2015).

[41] G. Bianconi and C. Rahmede, Scientific Reports **7** (2017).

[42] E. Heintze and H. Karcher, Ann. Sci. Ecole Norm. Sup **11**, 451 (1978).

[43] L. N. Vaserstein, Problemy Peredachi Informatsii **5**, 64 (1969).

[44] B. B. Bhattacharya and S. Mukherjee, Discrete Mathematics **338**, 23 (2015).

[45] J. Jost, *Riemannian Geometry and Geometric Analysis* (Springer, 7th ed., 2017).

[46] P. Erdős and A. Rényi, Bull. Inst. Internat. Statist **38**, 343 (1961).

[47] L. Šubelj and M. Bajec, The European Physical Journal B **81**, 353 (2011).

[48] J. Leskovec, J. Kleinberg, and C. Faloutsos, ACM Transactions on Knowledge Discovery from Data (TKDD) **1**, 2 (2007).

[49] R. Guimera, L. Danon, A. Diaz-Guilera, F. Giralt, and A. Arenas, Physical Review E **68**, 065103 (2003).

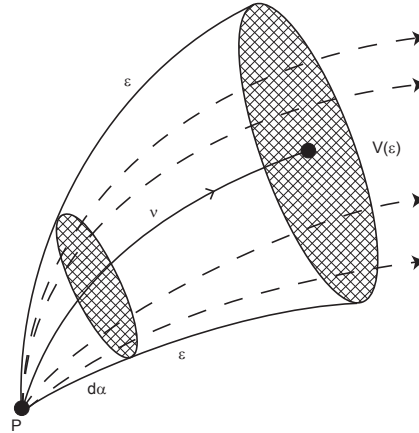


FIG. 1. The geometric interpretation of Ricci curvature. Ricci curvature measures the growth of volumes, more precisely, the growth of  $(n - 1)$ -dimensional solid angles in the direction of the vector  $\mathbf{v}$ . It also measures the dispersion rate of the family of geodesics with the same initial point, that are contained within the given solid angle. (In contrast, sectional curvature measures the divergence rate of pairs of geodesics starting from a common point, and contained within the solid angle, as a function of the initial angle made by the geodesics.)

- [50] M. E. Newman, *Physical Review E* **74**, 036104 (2006).
- [51] H. Jeong, S. P. Mason, A. L. Barabási, and Z. N. Oltvai, *Nature* **411**, 41 (2001).
- [52] T. Beuming, L. Skrabaneck, M. Y. Niv, P. Mukherjee, and H. Weinstein, *Bioinformatics* **21**, 827 (2005).
- [53] J. F. Rual, K. Venkatesan, T. Hao, T. Hirozane-Kishikawa, A. Dricot, N. Li, G. F. Berriz, F. D. Gibbons, M. Dreze, N. Ayivi-Guedehoussou, and *et al*, *Nature* **437**, 1173 (2005).
- [54] J. Kunegis, in *Proceedings of the 22nd international conference on World Wide Web companion* (2013) pp. 1343–1350.
- [55] L. C. Freeman, *Sociometry* , 35 (1977).
- [56] M. Girvan and M. Newman, *Proceedings of the National Academy of Sciences* **99**, 7821 (2002).
- [57] P. Marsden and K. Campbell, *Social forces* **63**, 482 (1984).
- [58] L. Backstrom and J. Kleinberg, in *Proceedings of the 17th ACM conference on Computer supported cooperative work & social computing* (ACM, 2014) pp. 831–841.
- [59] P. W. Holland and S. Leinhardt, *Comparative Group Studies* **2**, 107 (1971).
- [60] V. Latora and M. Marchiori, *Physical Review Letters* **87**, 198701 (2001).
- [61] M. J. . T. A. Pouryahya, M., arXiv **arXiv:1712.02943** (2017).

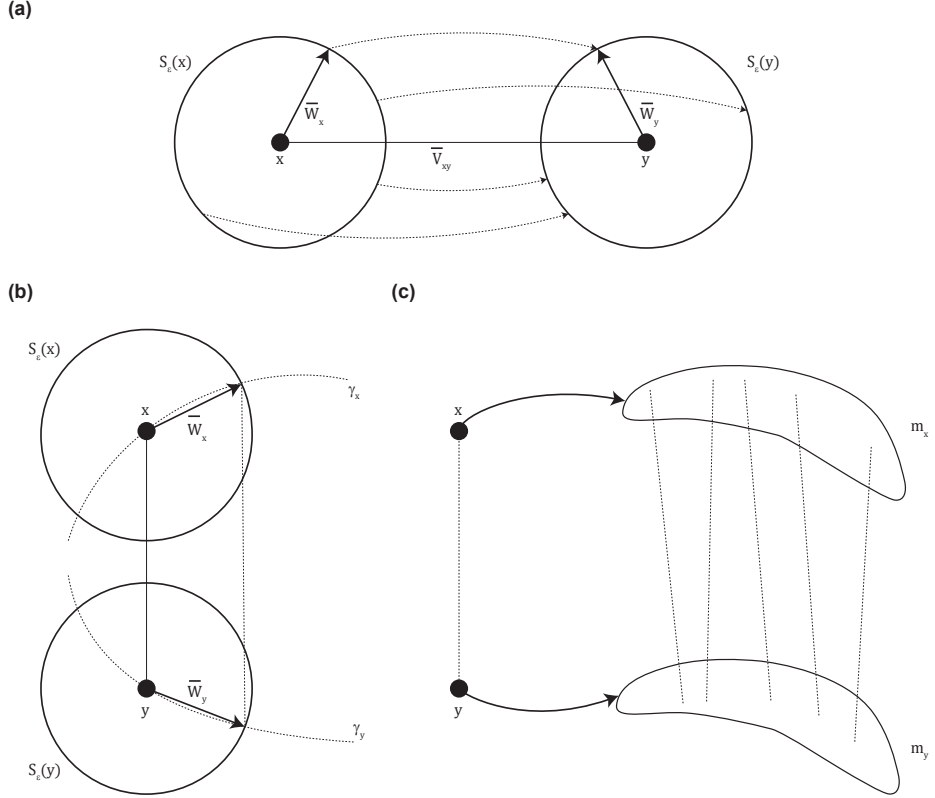


FIG. 2. The interpretation of Ollivier-Ricci curvature. (a) Given two close points  $x$  and  $y$  in a Riemannian manifold of dimension  $n$ , defining a tangent vector  $\bar{v}_{xy}$ , one can consider the parallel transport in the direction  $\bar{v}_{xy}$ . Then points on a infinitesimal sphere  $S_\varepsilon(x)$  centered at  $x$ , are transported to points on the corresponding sphere  $S_\varepsilon(y)$  by a distance equal to  $d(x, y) \left(1 - \frac{\varepsilon^2}{2n} \text{Ric}(\bar{v}_{xy})\right)$ , on the average. It follows that in spaces of positive Ricci curvature spheres are closer than their centers, while in spaces of negative curvature they are farther away. (b) In Riemannian manifolds of positive (respectively, negative) curvature, balls are closer (respectively, farther) than their centers. (c) To generalize this idea to metric measure spaces, one has to replace the (volumes of) spheres or balls, by measures  $m_x, m_y$ . Points will be transported by a distance equal to  $(1 - \kappa)d(x, y)$ , on the average, where  $\kappa = \kappa(x, y)$  represents the coarse (Ollivier) curvature along the geodesic segment  $xy$ . This illustration is an adaptation of the original figure in [17].

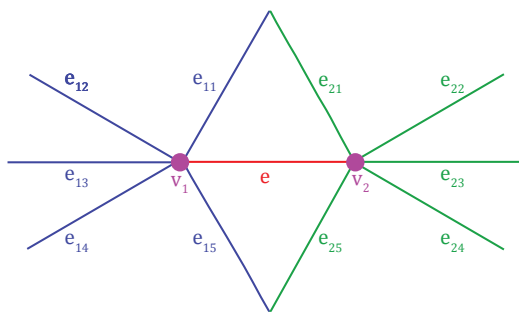


FIG. 3. Forman-Ricci curvature of an edge  $e$  connecting the vertices  $v_1$  and  $v_2$  and contribution from edges parallel to the edge  $e$  under consideration. An edge is said to be parallel to a given edge  $e$ , if it has in common with  $e$  either a “child” (i.e., a lower dimensional face), or a “parent” (i.e., a higher dimensional face), but not both simultaneously. The edges  $e_{11}, \dots, e_{15}$  are parallel to  $e$  because they share the vertex  $v_1$ , while the edges  $e_{21}, \dots, e_{25}$  are parallel to  $e$  because they share the vertex  $v_2$ .

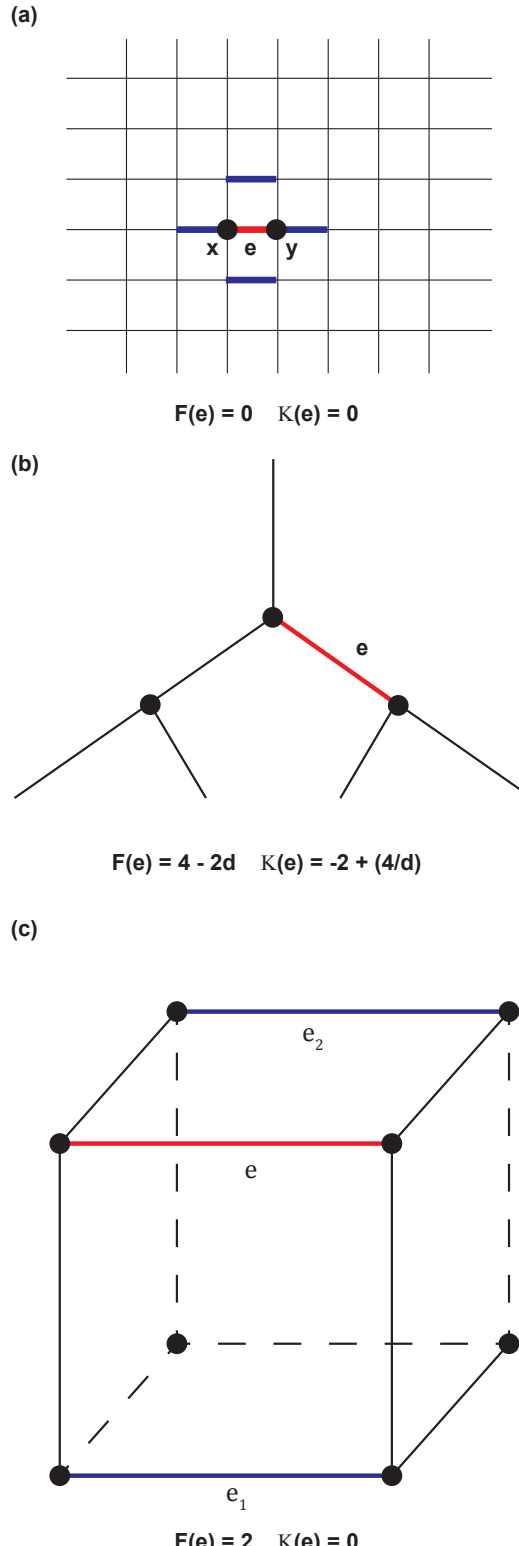


FIG. 4. Comparison of the Forman-Ricci (FR) and Ollivier-Ricci (OR) curvatures in simple yet important types of networks: (a) Square grid. (b) Regular tree. (c) Cube. Here the non-lazy random walk was used to compute Ollivier-Ricci curvature.

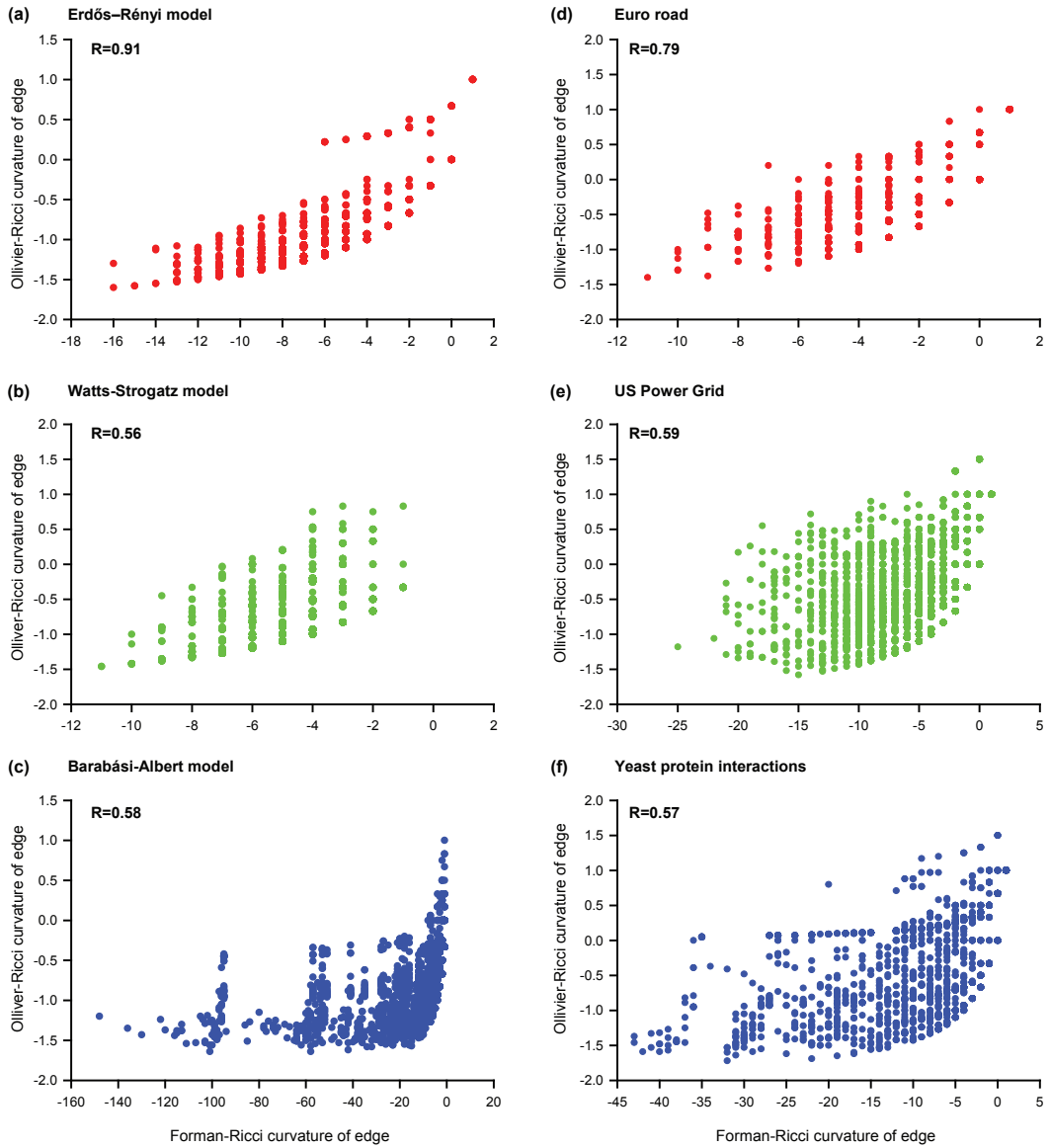


FIG. 5. Correlation between Forman-Ricci (FR) and Ollivier-Ricci (OR) curvature of edges in model and real networks. (a) Erdős-Rényi (ER) model. (b) Watts-Strogatz (WS) model. (c) Barabási-Albert (BA) model. (d) Euro road. (e) US Power Grid. (f) Yeast protein interactions. We indicate the Spearman correlation coefficient  $R$  in each plot.

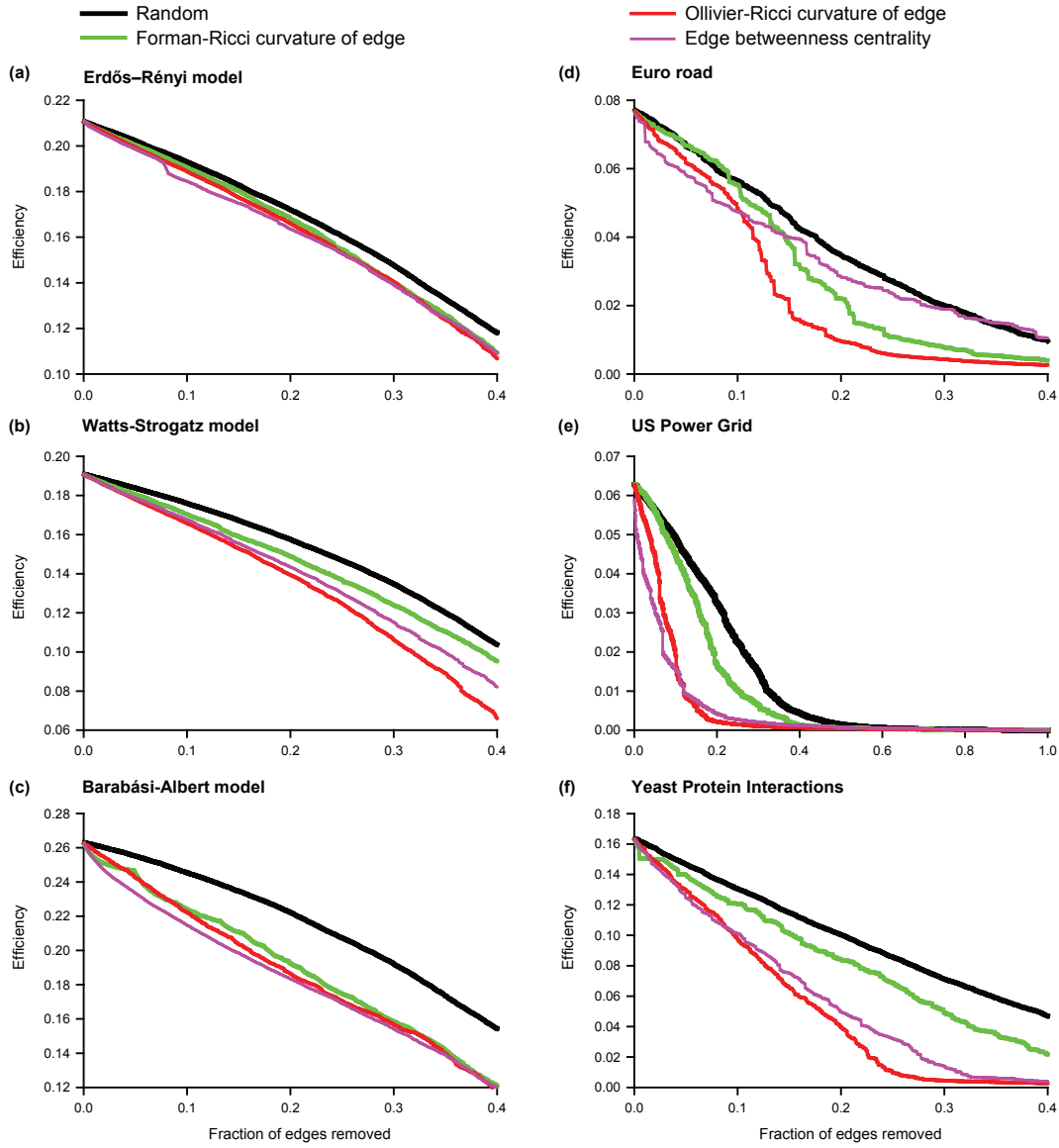


FIG. 6. Communication efficiency as a function of the fraction of edges removed in model and real networks. (a) Erdős-Rényi (ER) model. (b) Watts-Strogatz (WS) model. (c) Barabási-Albert (BA) model. (d) Euro road. (e) US Power Grid. (f) Yeast protein interactions.

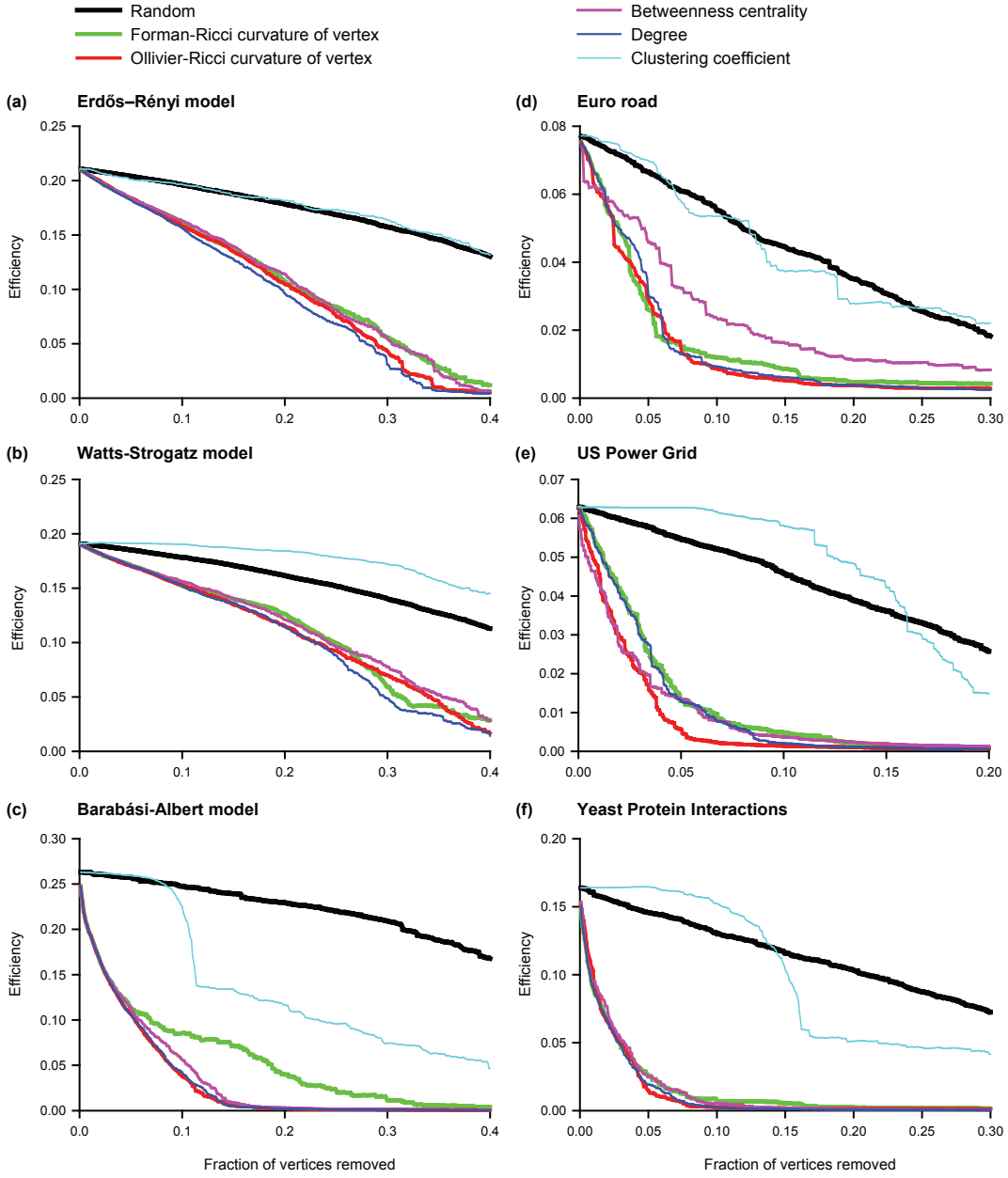


FIG. 7. Communication efficiency as a function of the fraction of vertices removed in model and real networks. (a) Erdős-Rényi (ER) model. (b) Watts-Strogatz (WS) model. (c) Barabási-Albert (BA) model. (d) Euro road. (e) US Power Grid. (f) Yeast protein interactions.

TABLE I. Comparison between Forman-Ricci (FR) and Ollivier-Ricci (OR) curvature of edges and vertices in model and real networks. In this table, we report the Spearman correlation between the two curvatures in each network.

Network	Correlation between FR and OR curvature of edges	Correlation between FR and OR curvature of vertices
<b>Model networks</b>		
Erdős-Rényi (ER) model with $p = 0.003$	0.91	0.98
Watts-Strogatz (WS) model with $k = 5$ and $p = 0.5$	0.56	0.83
Barabàsi-Albert (BA) model with $m = 3$	0.58	0.57
<b>Real networks</b>		
Euro Road	0.79	0.88
US Power Grid	0.59	0.68
Email communication	0.19	0.79
Hamsterster friendship	0.41	0.53
Adjective-Noun adjacency	0.15	0.47
Yeast protein interactions	0.57	0.79
PDZ domain interactions	0.59	0.88
Human protein interactions	0.49	0.83

TABLE II. Comparison of Forman-Ricci (FR) and Ollivier-Ricci (OR) curvature of edges with other edge-based measures in model and real networks. In this table, we report the Spearman correlation between edge-based measures and curvatures in each network.

Network	FR curvature with			OR curvature with		
	Edge betweenness	Edge embeddedness	Dispersion	Edge betweenness	Edge embeddedness	Dispersion
<b>Model networks</b>						
Erdős-Renyi (ER) model with $p = 0.003$	-0.80	0.03	0.0	-0.85	0.07	0.0
Watts-Strogatz (WS) model with $k = 5$ and $p = 0.5$	-0.67	-0.09	-0.08	-0.88	0.62	0.21
Barabàsi-Albert (BA) model with $m = 3$	-0.83	-0.41	-0.27	-0.65	0.01	0.01
<b>Real networks</b>						
Euro Road	-0.31	-0.31	-0.07	-0.50	0.08	0.03
US Power Grid	-0.26	-0.41	-0.19	-0.61	0.16	0.06
Email communication	-0.32	-0.45	-0.40	-0.61	0.55	0.24
Hamsterster friendship	-0.40	-0.39	-0.28	-0.70	0.43	-0.01
Adjective-Noun adjacency	-0.42	-0.72	-0.55	-0.51	0.22	0.09
Yeast protein interactions	-0.32	-0.15	-0.09	-0.76	0.06	0.01
PDZ domain interactions	-0.34	0.01	0.0	-0.74	-0.02	0.0
Human protein interactions	-0.40	-0.23	-0.09	-0.48	0.04	0.07

TABLE III. Comparison of Forman-Ricci (FR) and Ollivier-Ricci (OR) curvature of vertices with other vertex-based measures in model and real networks. In this table, we report the Spearman correlation between vertex-based measures and curvatures in each network.

Network	FR curvature with			OR curvature with		
	Degree	Clustering coefficient	Betweenness centrality	Degree	Clustering coefficient	Betweenness centrality
<b>Model networks</b>						
Erdős-Rènyi (ER) model with $p = 0.003$	-0.94	-0.01	-0.94	-0.94	0.04	-0.93
Watts-Strogatz (WS) model with $k = 5$ and $p = 0.5$	-0.96	-0.18	-0.91	-0.83	0.29	-0.96
Barabási-Albert (BA) model with $m = 3$	-0.68	-0.48	-0.84	-0.94	-0.21	-0.86
<b>Real networks</b>						
Euro Road	-0.82	-0.39	-0.57	-0.82	-0.21	-0.71
US Power Grid	-0.79	-0.49	-0.62	-0.68	0.02	-0.80
Email communication	-0.97	-0.31	-0.57	-0.80	0.06	-0.88
Hamsterster friendship	-0.94	0.32	-0.71	-0.43	0.72	-0.67
Adjective-Noun adjacency	-0.96	-0.50	-0.84	-0.57	0.07	-0.76
Yeast protein interactions	-0.57	-0.33	-0.54	-0.58	-0.04	-0.71
PDZ domain interactions	-0.59	0.13	-0.63	-0.53	-0.11	-0.62
Human protein interactions	-0.69	-0.44	-0.66	-0.82	-0.35	-0.83